AJNR

MR Angiography of the Great Anterior Radiculomedullary Artery (Adamkiewicz Artery) Validated by Digital Subtraction Angiography

R.J. Nijenhuis, M. Mull, J.T. Wilmink, A.K. Thron and W.H. Backes

R.J. Nijenhuis
M. Mull
J.T. Wilmink
A.K. Thron
W.H. Backes

MR Angiography of the Great Anterior Radiculomedullary Artery (Adamkiewicz Artery) Validated by Digital Subtraction Angiography

BACKGROUND AND PURPOSE: Imaging of the anterior superficial spinal cord arteries by MR angiography is hindered by their small calibers and the similarity in configuration with the anterior superficial spinal cord veins. To validate the location and spatial configuration of the great anterior radiculomedullary artery, (ie, the Adamkiewicz artery [AKA]), contrast-enhanced MR angiography (CE-MRA) was compared with digital subtraction angiography (DSA).

METHODS: Fifteen patients with suspected spinal cord vascular pathology underwent both spinal CE-MRA and selective spinal DSA. Two phase CE-MRA was performed with the use of a centric *k*-space filling scheme synchronized to the contrast bolus arrival. The level and side of the AKA origin were scored on the DSA and CE-MRA images and compared regarding image quality in terms of vessel conspicuity, contrast, continuity, sharpness, and background homogeneity on a relative 5-point scale.

RESULTS: Localization and spatial configuration of the AKA by CE-MRA was in agreement with DSA findings in 14 of 15 cases. One mismatch of 1 vertebral level (not side) appeared as a result of the tangled vascular pathology. Comparison of image quality revealed that DSA is superior to CE-MRA concerning vessel continuity, sharpness, and background homogeneity ($P < .001$). Overall vessel conspicuity and contrast were judged to be similar.

CONCLUSION: CE-MRA can visualize and localize the level of the AKA correctly. Image quality of CE-MRA is sufficient for detection of the AKA but is inferior to DSA.

Because of its high spatial resolution, digital subtraction angiography (DSA) is considered the standard of reference for imaging the very small anterior superficial spinal cord arteries. DSA is an invasive technique, however, in that it involves selective catheterization and contrast injection into small arteries supplying the spinal cord. This prompts the development of less invasive techniques such as CT angiography (CTA)[1-3] and MR angiography (MRA).[3-18] Before introducing these new techniques in a clinical setting it is of absolute importance to validate them.

Imaging of the anterior superficial spinal cord arteries requires simultaneous high spatial and high temporal resolution. The artery that is mainly responsible for the blood supply to the anterior spinal artery (ASA) and thus for the function of the thoracolumbar spinal cord is the great anterior radiculomedullary artery (ie, the Adamkiewicz artery [AKA]).[19,20] Although this is a minute artery (caliber 0.5–1.0 mm),[21] it is the largest anterior spinal cord artery. The intervertebral foramen at which the spinal branch of the posterior segmental artery enters the spinal canal and continues as the AKA displays considerable anatomic variance.[22] In addition, when a spinal vascular malformation (SVM) is to be diagnosed, the entire vertebral column has to be depicted, because an SVM can arise along this entire region.[22] This variability in vascular anatomy and pathology necessitates the use of a large field of view and thereby precludes achievement of high spatial reso-

lution. The short transit time from arteries to veins of the spinal cord circulation (<10 seconds),[15] as well as the spatial similarity in configuration of the anterior spinal cord arteries and veins (Fig 1), places further high demands on the temporal resolution of the imaging technique to obtain separation between arteries and veins.

First-pass contrast-enhanced MR angiography (CE-MRA) has been shown to visualize the AKA.[4-8] However, DSA verification has only been performed in a few cases.[6,7] Therefore, a systematic validation is of interest. The aim of the current study was to investigate whether 2-phase CE-MRA is able to detect and localize the AKA with DSA as the standard of reference in patients with suspected spinal cord vascular pathology.

Materials and Methods

Patients

From December 2003 through October 2004, 15 consecutive patients (12 men, 3 women) with suspected spinal vascular abnormalities were included in this study. The mean age was 60 years (range, 43–76 years). All patients underwent both CE-MRA and DSA investigation as part of the normal clinical work-up. Classification of vascular pathology, as listed in Table 1, was determined on the basis of DSA. Informed consent was obtained from all patients. CE-MRA was performed 1 day before DSA in all patients.

Imaging Modalities

CE-MRA. Imaging was performed on a clinical 1.5T MR imaging system equipped with a phased-array synergy surface spine coil. Patients were imaged in the supine position. The MR imaging protocol comprised 3 different pulse sequences. First, a T2-weighted survey scan was acquired to image the spinal cord and vertebral column for anatomic reference. The field of view (FOV) extended from the third
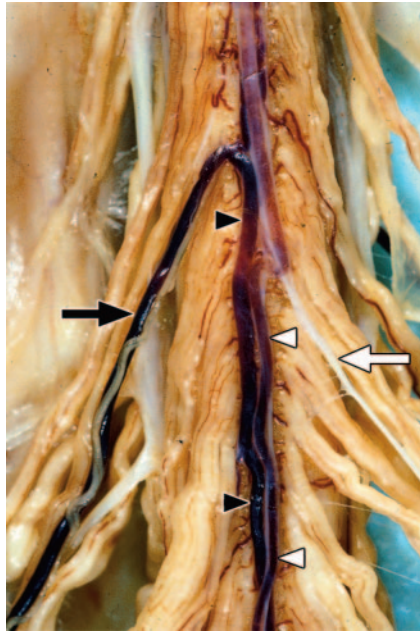
Fig 1. Postmortem spinal cord specimen of the anterior cord surface, on which both the superficial spinal cord arteries and veins are shown. The great anterior radiculomedullary artery (ie, the Adamkiewicz artery [AKA]) (*white arrow*) and anterior spinal artery (ASA) (*white arrowheads*) are displayed on the right side of the image. The anterior median vein (AMV) (*black arrowheads*) as well as the great anterior radiculomedullary vein (GARV) (*black arrow*) are displayed on the left side. Note the close anatomic relation between the AMV and ASA as well as the similarity in the configuration of the AKA and GARV, respectively. Clotted blood is present in the veins and ASA. No blood is present in the AKA (*white appearance*) because of the preparation process. (Used with permission.)

via the left antecubital vein. The test bolus was administered at the same injection rate of 3 mL/s as the final bolus using a power-injector followed by a saline flush of 25 mL. The MR fluoroscopy sequence consisted of an 80-mm section that was sagittally positioned through the aorta. This section was acquired once each second over a period of 2 minutes. The pulse sequence parameters were TR, 5.2 ms; TE, 1.4 ms; FA, 35°; FOV, 450 mm; and matrix, 205 × 256. Viewing the series of bolus timing images, the scan delay was defined as the time between start of test bolus injection and maximal enhancement of the entire aorta down to the bifurcation. The obtained scan delay was used to synchronize the sampling of the center of *k*-space with the peak contrast agent enhancement in the subsequent CE-MRA acquisition.

Third, for the final CE-MRA, a total volume of 45 mL (0.3 mmol/kg of body weight) of contrast agent was administered and flushed with 25 mL of saline both injected at a rate of 3 mL/s. The CE-MRA consisted of 2 consecutive dynamic phases to obtain an early (ie, first, preferably arterial) phase and a late (ie, second, combined arterial venous) phase 3D image set. Each phase took 36 to 41 seconds, depending on the number of sagittal sections required to cover the entire transverse cross-section of the vertebrae along the entire vertebral column. Sagittal section orientation was preferred over coronal orientation to obtain the least number of phase encoding steps and consequently the shortest acquisition time. The FOV in craniocaudal (read-out) direction was set to 500 mm to enable the maximum possible anatomic coverage to include (1) the (possibly aberrant) origin of the AKA and (2) the origin of any possible vascular abnormality. The FOV was 175 mm in anteroposterior (phase-encoding) direction (rectangular FOV of 35%). The use of a smaller FOV in the phase-encoding direction reduced the number of phase-encoding steps and therefore acquisition time. Matrix dimensions were 464 × 512 (phase encoding × read-out), and pixel size was 0.8 × 0.8 mm. Acquired sagittal sections were 1.2 mm and interpolated (zero-filling in *k*-space) during reconstruction to 0.6-mm sections. The number of sections was individually adjusted (range, 75–85; 45–51 mm) to include the entire vertebral column from T3 down to S5 in the craniocaudal direction. Acquisition parameters for the spoiled gradient-echo pulse sequence were TR, 5.9 ms; TE, 1.9 ms (partial echo, 65%); and FA, 30°. To obtain images in which venous enhancement was

thoracic vertebra (T3) to the fifth sacral vertebra (S5). Acquisition parameters were repetition time (TR), 2686 ms; echo time (TE), 120 ms; flip angle (FA), 90°; craniocaudal FOV, 500 mm; matrix, 320 × 480 (phase encoding × read-out); 12 sagittal sections; and voxel sizes, 1.25 × 1.67 × 4.0 mm.

Second, MR fluoroscopy was used to determine the scan delay between the start of contrast bolus injection and the start of the CE-MRA pulse sequence. For this purpose, a test bolus of 2.0 mL of gadopentetate dimeglumine (0.5 mol/L Gd-DTPA) was administered

Table 1: Patient characteristics and observations for contrast-enhanced magnetic resonance angiography and digital subtraction angiography

| Patient No./ Sex/Age (y) | CE-MRA | | | | | DSA | | | | |
| | AKA | | Other | GARV | | AKA | | Other | GARV | |
	Level	Side	ARA	Level	Side	Level	Side	ARA		Pathology
1/M/44	T9	Right	No	L2	Right	T9	Right	T4	No	Hemangioblastoma
2/M/62	T8	Left	No	L3	Right	T8	Left	No	No	SDAVF
3/M/57	L1	Right	No	No	No	L1	Right	No	No	SAVM, fistulous type
4/M/63	T9	Left	No	L1	Right	T9	Left	No	No	Spinal SAH
5/M/73	T12	Left	No	L3	Right	T12	Left	T3	No	None
6/M/64	T12	Left	No	L2	Left	T12	Left	No	No	SDAVF
7/M/48	T11	Left	No	L3	Right	T11	Left	No	No	SDAVF
8/M/55	L1	Right	No	L3	Right	L1	Right	No	No	SDAVF
9/M/72	T11	Left	No	L2	Right	T11	Left	No	No	SDAVF
10/M/66	L2	Left	No	L2	Right	L2	Left	No	No	SDAVF
11/F/43	T12	Left	No	No	No	L1	Left	No	No	SAVM, fistulous type
12/F/43	T11	Right	No	L3	Left	T11	Right	No	No	None
13/M/73	T10	Left	No	L2	Right	T10	Left	No	No	SDAVF
14/F/76	T12	Right	No	L3	Right	T12	Right	No	No	SDAVF
15/M/59	L1	Left	No	L2	Right	L1	Left	No	No	None

Note:—CE-MRA indicates contrast-enhanced magnetic resonance angiography; DSA, digital subtraction angiography; AKA, Adamkiewicz artery; ARA, anterior radiculomedullary artery; GARV, great anterior radiculomedullary vein; T, thoracic; L, lumbar; SDAVF, spinal dural arteriovenous fistula; SAVM, spinal arteriovenous malformation; SAH, subarachnoid hemorrhage. For a description of the present spinal vascular pathology, we refer to the existing literature.[30]
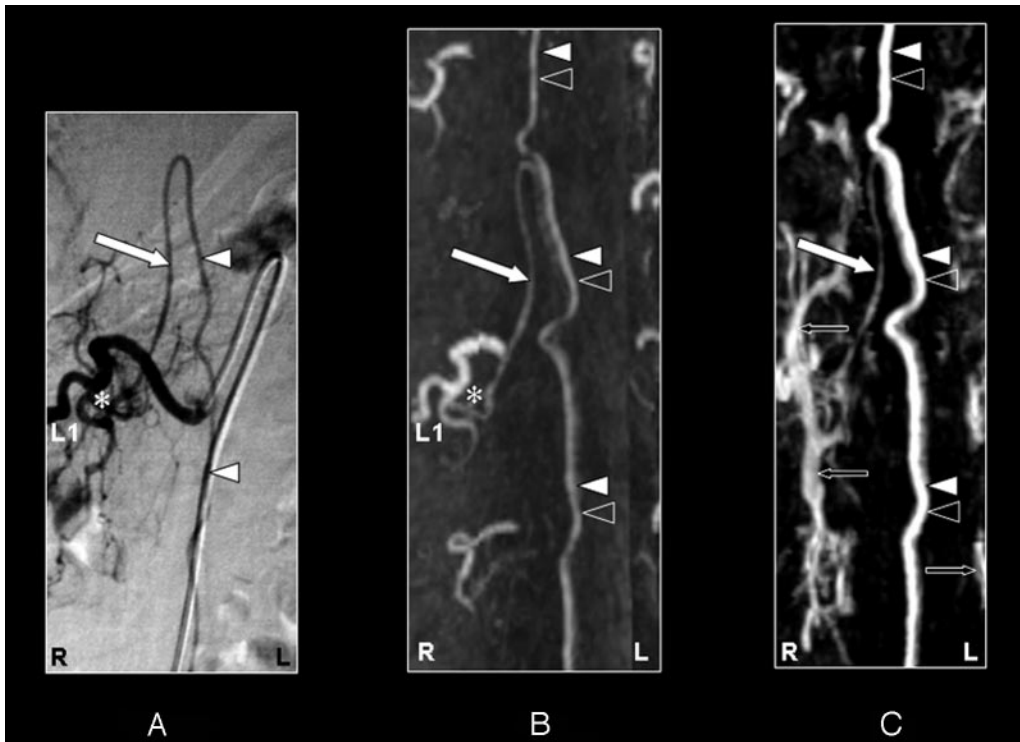
Fig 2. Coronal digital subtraction angiography (DSA) projection (*A*) and multiplanar reformatted contrast-enhanced MR angiography (CE-MRA) of the early phase (*B*) and late phase (*C*) in a 57-year-old male patient (case 3) with a spinal arteriovenous malformation (diagnosed on the basis of DSA). On the DSA projection image (*A*), the supplying segmental artery (SA) (*asterisk*), the great anterior radiculomedullary artery, (ie, the Adamkiewicz artery [AKA]) (*large white arrow*), and the anterior spinal artery (ASA) (*white arrowheads*) are shown. The CE-MRA of the early phase (*B*) shows the supplying SA (*asterisk*) and the AKA (*large white arrow*). Regarding the anterior midline enhancement in the early phase (*B*) above as well as below the connection of the AKA with the ASA, this is most likely to be enhancement of both the ASA (*white arrowheads*) and the anterior median vein (AMV) (*black arrowheads*). The late phase CE-MRA (*C*) shows diminished signal intensity of the AKA (*large white arrow*), in contrast to the anterior midline enhancement, which is clearly increased compared with the early phase (*B*) because of increased venous enhancement. The midline enhancement seen in the late phase (*C*) is most likely to be a combination of AMV (*black arrowheads*) and ASA (*white arrowheads*) enhancement. Furthermore, there is enhancement of the venous plexus (*small black arrows*) in the late phase (*C*) that is not seen in the early-phase CE-MRA image (*B*). Note that the cephalad enhancement above the connection of the AKA with the ASA is depicted only in the CE-MRA images (*B* and *C*), and not in the DSA image (*A*). Note also that the AKA appears enlarged in the DSA as well as the CE-MRA examination.

suppressed, *k*-space was filled using (elliptical) centric ordering in which the first 4 seconds were randomly filled. Imaging was performed without breath-hold.

DSA. Selective spinal DSA was performed by a transfemoral approach. In the frontal view, 2 frames per second were acquired. The manually injected contrast agent (2–3 mL per injection) had an iodine concentration of 300 mg of iodine/mL. Radiographic parameters were 80 kV; 400 mA; matrix, 1024 × 1024; entrance format, 11 × 13 cm; and spatial resolution, 2.2 line pairs/mm. Oblique views were added to elucidate the composition of the fistula zone in case of a spinal dural arteriovenous fistula (SDAVF). For image comparison with first-phase CE-MRA images, only early (arterially) enhanced images were used. The angiographic protocol was adapted to the underlying vascular pathology. In all cases, spinal DSA included identification of the arteries supplying the thoracolumbar region. Classification of pathologic findings was based on DSA findings.

Image Analysis

Postprocessing. The CE-MRA images were postprocessed using multiplanar reformations (MPR). One creator determined the level and side of the AKA. In addition, this creator provided a single digital first phase MRA image in which the AKA was optimally displayed for the consensus comparison study with DSA. Only one creator was used to prepare high-quality MRA images of the spinal vasculature for the comparison study. Localization of the AKA could be performed within 15 minutes. However, to optimally display the entire AKA from its origin of the posterior segmental artery (SA) to its connection and continuation to the ASA took 1–2 hours because the course of the AKA and its continuation are not situated in a single plane, and therefore (locally variably) curved MPR images had to be created. DSA images were printed on film.

Vessel Identification. The following criteria were applied to identify the AKA, the segmental origin of the AKA, and the great anterior radiculomedullary vein (GARV) on the first- and second-phase CE-MRA images: (1) an enhancing vessel observed in the first phase coursing through the intervertebral foramen toward the spinal cord, with a steep ascending course and connecting to the midline vessel on the anterior spinal cord surface, that did not enhance more intensely in the second phase was considered to be the AKA. (2) If an enhanced vessel was observed in the first phase that coursed from the spinal cord toward an intervertebral foramen, with a descending course and connected to the midline vessel on the anterior spinal cord surface, that did not enhance less intensely in the second phase, or was observed only in the second phase, this vessel was considered to be the GARV. (3) The segmental level of origin of the AKA and GARV was confirmed with the use of the T2-weighted anatomic images. The intervertebral foramen at which the spinal branch of the posterior SA entered the spinal canal and continued as the AKA was determined as the level of origin of the AKA. For instance, in case the spinal branch entered between T12 and L1, it was considered to be the segmental level T12. (4) If more enhancing vessels were observed in the first-phase CE-MRA images that originated from an intervertebral foramen between T9 and L2 and continued toward the midline vessel on the anterior spinal cord surface, the one with the largest (ie, widest) diameter was considered to represent the AKA and arteries of smaller diameter (ie, thinner) were considered to be other anterior radiculomedullary arteries (ARAs). Vascular pathology was also investigated by DSA and CE-MRA but is outside the scope of the current article and will be reported elsewhere.

Image Quality Measurements. Three experienced neuroradiologists jointly scored the following aspects of the images of both CE-MRA and DSA: (1) level, side, and similarity in configuration of the
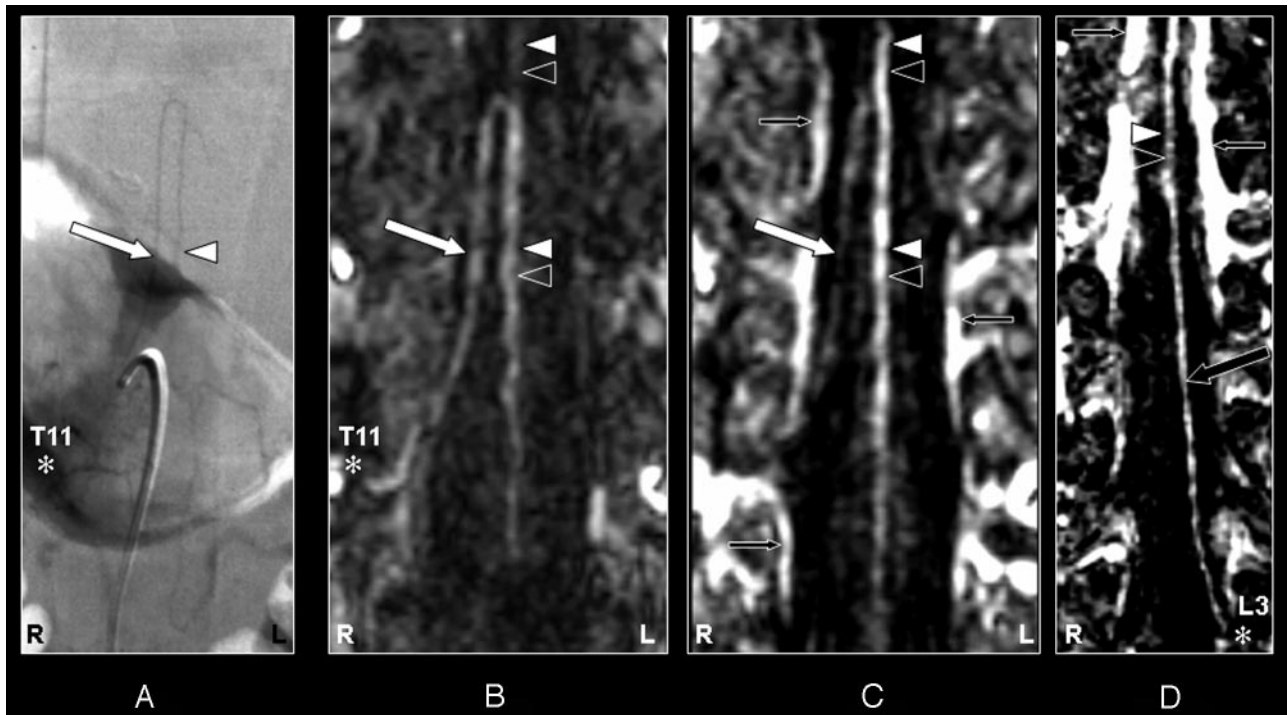
Fig 3. Coronal digital subtraction angiography (DSA) projection (*A*) and multiplanar reformatted contrast-enhanced MR angiography (CE-MRA) of the early phase (*B*) and late phase (*C* and *D*) in a 43-year-old female patient (case 12) with no spinal arteriovenous malformations. On the DSA projection image (*A*), the supplying segmental artery (SA) (*asterisk*), the great anterior radiculomedullary artery (ie, the Adamkiewicz artery [AKA]) (*large white arrow*), and the anterior spinal artery (ASA) (*white arrowhead*) are shown. The CE-MRA of the early phase (*B*) shows the supplying SA (*asterisk*) and the AKA (*large white* arrow). Regarding the anterior midline enhancement in the early phase (*B*) above as well as below the connection of the AKA with the ASA, this is most likely to be the combined enhancement of the ASA (*white arrowheads*) as well as the anterior median vein (AMV) (*black arrowheads*). The late phase CE-MRA (*C*) shows diminished signal intensity of the AKA (*large white arrowhead*) in contrast to the anterior midline enhancement, which is clearly increased compared with the early phase (*B*) because of increased venous enhancement. The midline enhancement seen in the late phase (*C* and *D*) is most likely to be a combination of AMV (*black arrowheads*) and ASA (*white arrowheads*) enhancement. In addition, the great anterior radiculomedullary vein (GARV) (*large black arrow*) is displayed in the late phase of the CE-MRA (*D*). Note that the signal intensity of the GARV and midline enhancement is equal (*D*). Furthermore, there is enhancement of the venous plexus (*small black arrows*) in the late phase (*C* and *D*) that is not seen in the early-phase CE-MRA image (*B*). Furthermore, note that the cephalad enhancement above the connection of the AKA with the ASA is depicted only in the CE-MRA images (*B* and *C*), and not in the DSA image (*A*).

AKA, (2) depiction of additional ARAs, and finally (3) image quality regarding background homogeneity, vessel sharpness, continuity, conspicuity, and contrast on a relative 5-point scale. Interpretation of relative scores was as follows: −2 when DSA was clearly superior to CE-MRA; −1 when DSA was marginally superior to CE-MRA; 0 for equal appearance; +1 when CE-MRA was marginally superior to DSA; +2 when CE-MRA was clearly superior to DSA.

Statistical Analysis
For statistical analysis of the image quality comparisons the (nonparametric) Wilcoxon paired sample test was used.[23] To this end, the absolute values of the relative scores were ranked for each image quality item. The ranks for the cases where CE-MRA was better than DSA (ie, positive relative scores) and where DSA was better than CE-MRA (ie, negative relative scores) were separately summed (T$_+$ and T$_−$, respectively) and nonparametrically (2-tailed) tested to be different from the critical value (T$_{0.05, 15}$ = 25 for n = 15) of the Wilcoxon T distribution. Statistical significance was inferred when the *P* value obtained was less than .05.

Results
In all 15 patients, the AKA and its segmental origin were detected on both CE-MRA phases and on DSA (Figs 2–6). No adverse events occurred during or after any of the procedures. Table 1 summarizes the results of our patient group concerning lateralization and segmental origin of the AKA and GARV for CE-MRA and DSA.

The prospective localization and spatial configuration of the AKA as obtained by CE-MRA was in agreement with the DSA result in 14 of 15 cases (93%) (Figs 2–5). In 1 case (case 11), there was disagreement between the DSA (Fig 6*A*) and CE-MRA regarding the vertebral level (not side) of the SA connecting to the AKA because of the tangled vascular pathology of multiple veins near the AKA (Fig 6*B*). The correct segmental origin could retrospectively be identified for this case (Fig 6*C*). The AKA derived from the left side in 10 patients (67%) and from the right side in 5 patients (33%). The AKA appeared enlarged in 2 patients (Figs 2 and 6) because of the underlying pathology (spinal arteriovenous malformation). An additional ARA was found in 2 cases by DSA but not by CE-MRA (Table 1).

In the second-phase images, the GARV could be detected and localized in 13 of 15 patients (Fig 3*D*, 4*D*, and 5*D*). This was in contrast to the DSA, where the GARV was not detected in any of the cases. Based on the localization of the GARV from the second phase CE-MRA images, retrospectively in 4 of 15 cases, the GARV was faintly visible in the first-phase images.

Image Quality Measurements
Comparison of image quality between CE-MRA and DSA (Table 2) revealed that DSA was superior to CE-MRA (*P* < .001) concerning vessel continuity, sharpness, and background homogeneity. Overall vessel conspicuity and contrast did not differ (*P* > .05).
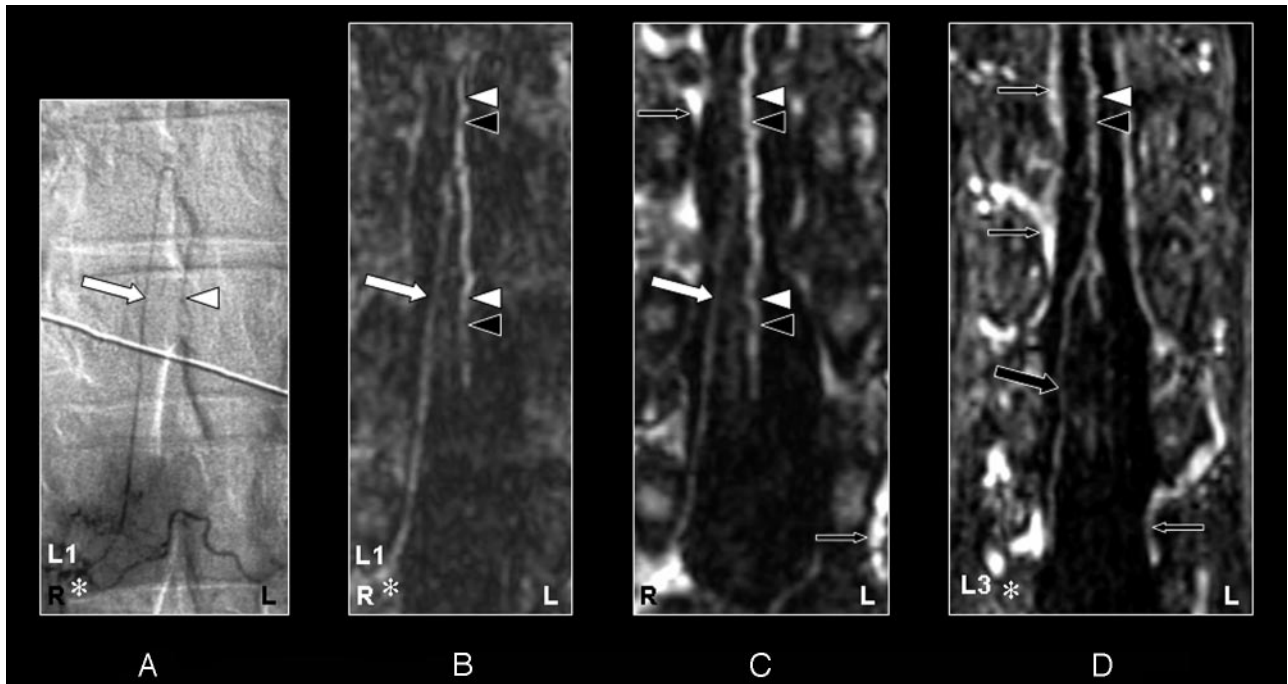
Fig 4. Coronal digital subtraction angiography (DSA) projection (*A*) and multiplanar reformatted contrast-enhanced MR angiography (CE-MRA) of the early phase (*B*) and late phase (*C* and *D*) in a 55-year-old male patient (case 8) with a spinal dural arteriovenous fistula (diagnosed on the basis of DSA). On the DSA projection image (*A*) the supplying segmental artery (SA) (*asterisk*), the great anterior radiculomedullary artery (ie, the Adamkiewicz artery [AKA]) (*large white arrow*), and the anterior spinal artery (ASA) (*white arrowhead*) are shown. The CE-MRA of the early phase (*B*) shows the supplying SA (*asterisk*) and the AKA (*large white arrow*). Regarding the anterior midline enhancement in the early phase (*B*) above as well as below the connection of the AKA with the ASA, this is most likely to be enhancement of both the ASA (*white arrowheads*) and the anterior median vein (AMV) (*black arrowheads*). The late-phase CE-MRA (*C*) shows diminished signal intensity of the AKA (*large white arrow*), in contrast to the anterior midline enhancement, which is clearly increased compared with the early phase (*B*) as a result of increased venous enhancement. The midline enhancement seen in the late phase (*C* and *D*) is most likely to be a combination of AMV (*black arrowheads*) and ASA (*white arrowheads*) enhancement. In addition, the great anterior radiculomedullary vein (GARV) (*large black arrow*) is displayed in the late phase of the CE-MRA (*D*). Note that the signal intensity of the GARV and midline enhancement is equal (*D*). Furthermore, there is enhancement of the venous plexus (*small black arrows*) in the late phase (*C* and *D*), which is not seen in the early phase CE-MRA image (*B*). Note that the cephalad enhancement above the connection of the AKA with the ASA is only depicted on the CE-MRA images (*B* and *C*), and not in the DSA image (*A*). Note that there is more background enhancement in the CE-MRA images.

Discussion

In this study, 2-phase CE-MRA was compared with DSA for the detection and localization of the great anterior radiculomedullary artery (ie, the AKA) and to differentiate it from the GARV. The 2 most important aspects in MR angiography of the anterior superficial spinal cord arteries that determine the image result are spatial and temporal resolution. Achieving a high spatial resolution, which is required for visualization of the submillimeter-sized arteries (<1.0 mm), is hampered by the fact that a large field of view has to be used. Furthermore, when no clear temporal separation between the anterior superficial spinal cord arteries and veins is possible, no definitive judgment can be made whether a depicted vascular structure on the anterior spinal cord surface is arterial or venous, because the configuration and midline localization of the anterior superficial spinal cord veins and arteries is quite similar. The temporal resolution that has to be achieved is on the order of (or less than) 10 seconds, because this is the estimated arteriovenous window of the normal spinal circulation time that has been reported.[15]

Until now, several MRA techniques have been attempted to visualize the anterior superficial spinal cord arteries. The first techniques used were blood flow-dependent, such as 3D phase conventional angiography (3D PCA)[11,12,14] and 3D contrast-enhanced time-of-flight imaging (3D CE-TOF).[9,11,24] With 3D PCA, only an enlarged AKA could be depicted in the pathologic situation of increased flow as occurring in arterio-

venous malformations. However, no separation could be achieved between anterior superficial spinal cord arteries and veins. The greatest disadvantage of the 3D CE-TOF technique is the long acquisition time required (~10 minutes), resulting in substantial venous as well as background enhancement.[11,24] Despite the use of a contrast medium in 3D CE-TOF imaging, the anterior superficial spinal cord arteries were poorly resolved[9,11,24] because the larger veins may overshadow smaller neighboring arteries. To achieve a better arterial visualization without venous enhancement, first-pass MR imaging featuring a rapid injection of contrast medium and a high-speed sophisticated acquisition sequence has been proposed.[8,10,13,17,25] Using centric *k*-space sampling, Willinek et al[26] have shown that it is possible to achieve an effective temporal resolution of 5–10 seconds, though the actual total acquisition duration may be quite longer. In the current study, we have used the centric ordered *k*-space filling to enable an effective temporal resolution of 5–10 seconds that is devoted to the arterial phase. The remaining 31 seconds of the CE-MRA first-phase sequence, in which both arteries and veins are both filled with contrast agent, were used to increase spatial resolution (eg, delineation and sharpness of the enhanced vessels).

Although the GARV was already enhanced in the first-phase MR image in 4 of the 15 cases, we believe that the 2-phase CE-MRA approach enables a reliable differentiation between the AKA and GARV as the signal intensity of the GARV increases and that of the AKA decreases in the second-
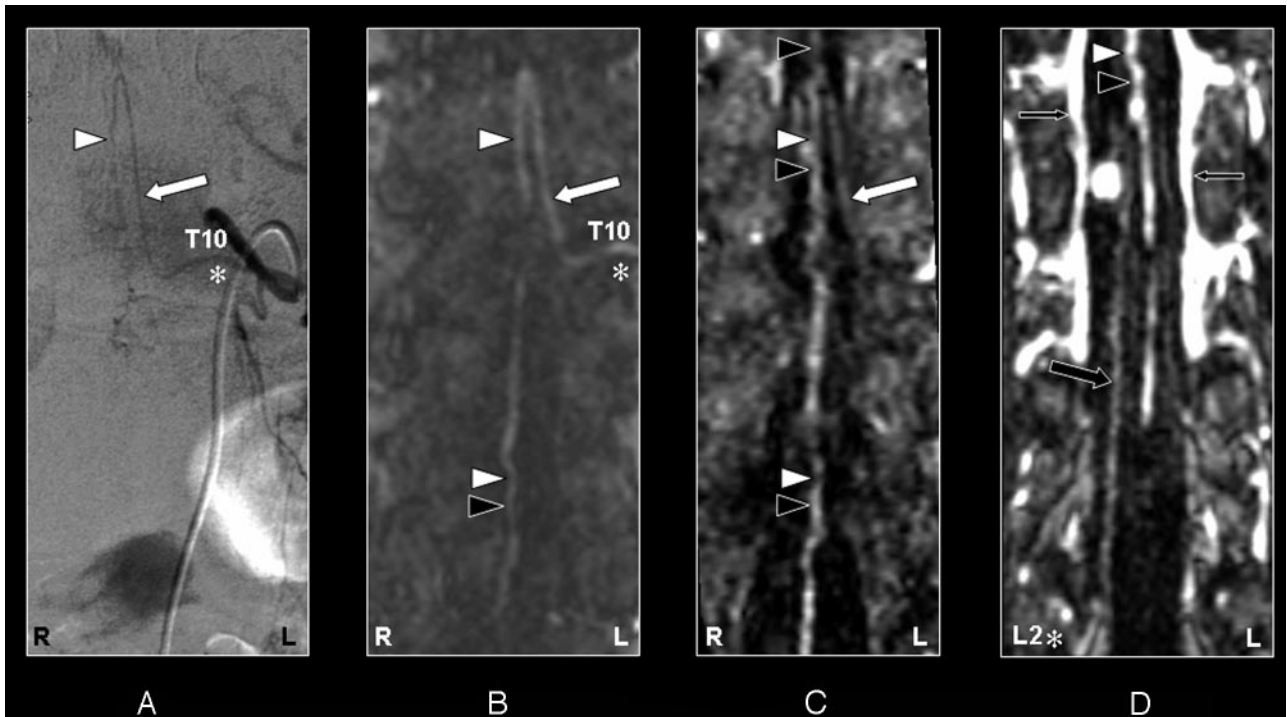
Fig 5. Coronal digital subtraction angiography (DSA) projection (*A*) and multiplanar reformatted contrast-enhanced MR angiography (CE-MRA) of the early phase (*B*) and late phase (*C* and *D*) in a 73-year-old male patient (case 13) with a spinal dural arteriovenous fistula (diagnosed on the basis of DSA). On the DSA projection image (*A*) the supplying segmental artery (SA) (*asterisk*), the great anterior radiculomedullary artery (ie, the Adamkiewicz artery [AKA]) (*large arrow*), and the anterior spinal artery (ASA) are shown. The CE-MRA of the early phase (*B*) shows the supplying SA (*asterisk*) and the AKA (*large white arrow*). Regarding the anterior midline enhancement in the early phase (*B*) above as well as below the connection of the AKA with the ASA, this is most likely to be enhancement of both the ASA (*white arrowheads*) as well as the anterior median vein (AMV) (*black arrowheads*). The late phase CE-MRA (*C*) shows diminished signal intensity of the AKA (*large white arrow*), in contrast to the anterior midline enhancement, which is clearly increased compared with the early phase (*B*) as a result of increased venous enhancement. The midline enhancement in the late phase (*C*) below the connection of the AKA with the ASA is most likely to be a combination of AMV (*black arrowheads*) and ASA (*white arrowheads*) enhancement. In addition, the great anterior radiculomedullary vein (GARV) (*large black arrow*) is displayed in the late phase of the CE-MRA (*D*). Furthermore, there is enhancement of the venous plexus (*small black arrows*) in the late phase, which is not seen in the early-phase CE-MRA image (*B*). Note that the cephalad enhancement above the connection of the AKA with the ASA is depicted only in the late phase CE-MRA (*C*) and is therefore most likely to correspond to enhancement of the AMV (*black arrowhead*) only.

phase compared with the first-phase CE-MRA images. Therefore, bolus arrival timed (ie, first-pass) imaging using centric ordered *k*-space filling is, in our experience, the best technique to obtain the necessary temporal resolution for arteriovenous separation of the AKA from the GARV. However, whether the current temporal resolution is sufficient to separate the ASA from the anterior median vein (AMV) remains doubtful, especially in cases with an aberrant spinal cord circulation. A limitation of the current study is therefore that the inclusion of patients with vascular spinal cord malformations complicates the separate depiction of the ASA and the AMV.

In addition, with noncentric ordered *k*-space filling, separation of arteries from veins seems possible as proved by Yamada et al.[6,7] They were the first to report on the visualization of the AKA using a CE-MRA technique with 2 dynamic phases and were able to distinguish the AKA from the GARV in some cases. However, the detection rate of the AKA in this study of 26 patients was only 69%, which is lower than in the current study, whereas DSA validation was performed in only 3 cases.

The present comparative study has shown that though the image quality of CE-MRA was found to be inferior to that of DSA, CE-MRA offers sufficient image (artery to background) contrast to consistently detect the AKA in patients with and without SVMs. In our patient population, there were 2 spinal arteriovenous malformations (SAVMs), 8 spinal dural arteriovenous fistulas (SDAVFs), 1 hemangioblastoma, and 1 spinal

subarachnoidal hemorrhage. Three patients had no pathologic conditions of the spinal vasculature. A SVM may affect the spinal circulation time. The arteriovenous window in a SAVM may be shortened, in contrast to an SDAVF, where it may be prolonged compared with normal spinal circulation.[27] Therefore, knowledge of the underlying circulation time seems to be important because this may influence the imaging time, especially for the filling of the *k*-space center. However, the exact period for shortening or prolongation of spinal cord circulation is unknown. Therefore, all patients were imaged with the same MR imaging protocol and the same criterion (complete aortic filling) for the scan delay. Regarding the possible suboptimal timings of the spinal cord artery filling and center of *k*-space acquisition, the presence of a pathologic vascular condition (except for 1 case) obviously did not impair AKA identification.

In 1 case, we obtained a mismatch of 1 vertebral level (not side) because of the tangle of multiple veins close to the AKA. The arteriovenous window for the SAVM apparently was too short to be separated by the MR acquisition technique used. However, as reported previously by others,[28] the subsequent DSA examination would still have been limited in procedure time and radiation dose, because adjacent levels are usually examined for pathologic conditions as well.

On the anterior spinal cord surface, cephalad enhancement above the connection of the AKA was found more often in first-phase CE-MRA than with early-phase DSA. Although
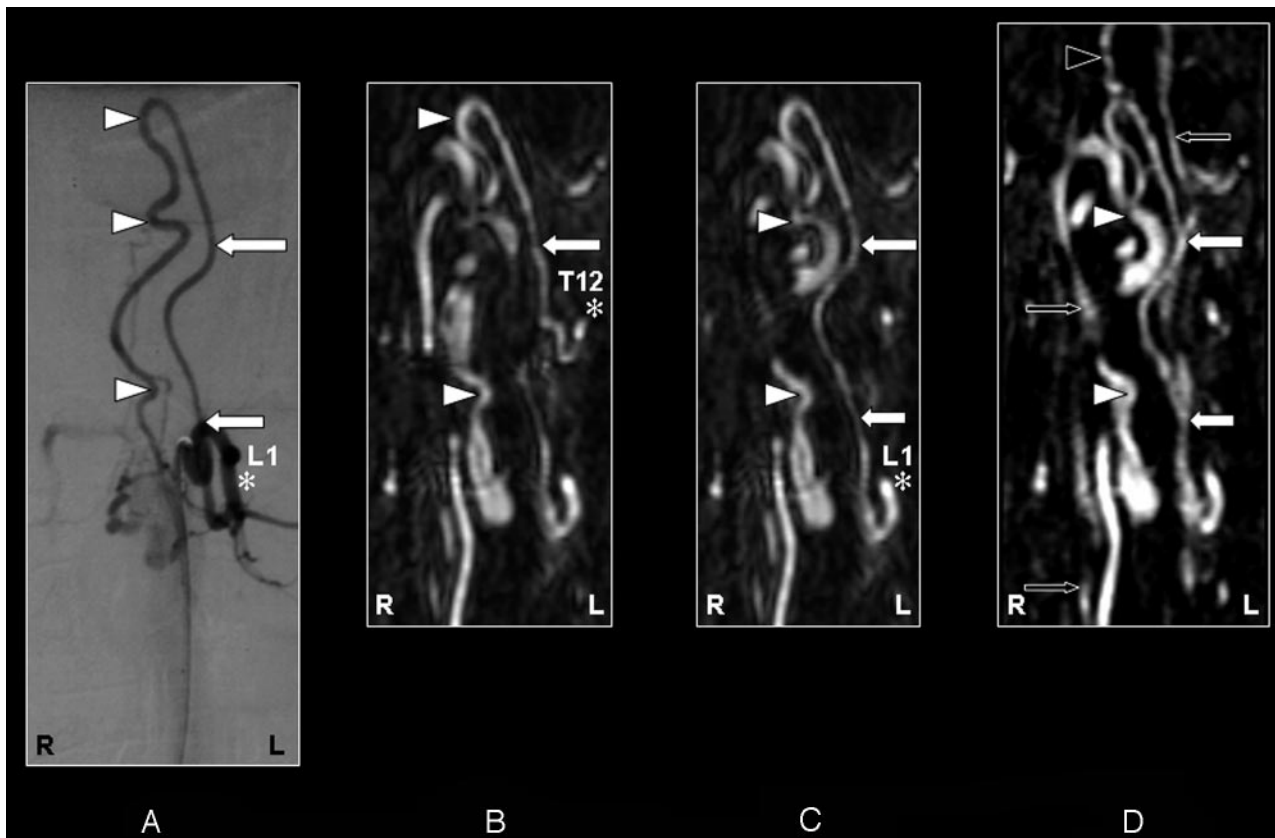
Fig 6. Coronal digital subtraction angiography (DSA) projection (*A*) and multiplanar reformatted contrast-enhanced MR angiography (CE-MRA) of the early phase (*B* and *C*) and late phase (*D*) of a 43-year-old female patient (case 11) with a perimedullary arteriovenous malformation of the fistulous type (diagnosed on the basis of DSA). On the DSA projection image (*A*), the supplying segmental artery (SA) (*asterisk*), the great anterior radiculomedullary artery (ie, the Adamkiewicz artery [AKA]) (*large white arrow*), and the anterior spinal artery (ASA) (*white arrowheads*) are shown. The SA (*asterisk*) connecting to the AKA (*large arrow*) is falsely identified in the early phase CE-MRA (*B*) because of an erroneously created curved multiplanar reformation resulting from the many entangled vessels. Retrospectively, the correct SA (*asterisk*) supplying the AKA (*large white arrows*) was identified in the early-phase CE-MRA (*C*). The cephalad enhancement above the connection of the AKA (*large white arrows*) with the ASA is depicted only in the late phase CE-MRA image (*D*), and therefore is most likely to represent the anterior median vein (*black arrowhead*). In addition, there is enhancement of the venous plexus (*small black arrows*) in the late-phase CE-MRA image (*D*) that is not seen in the early phase CE-MRA image (*B* and *C*). Note the strong enhancement of the dilated and arterialized veins on the CE-MRA images, which is due to the nonselective manner of contrast administration. Furthermore, the AKA appears enlarged in the DSA as well as the CE-MRA examination.

Table 2: Comparison of image quality between contrast-enhanced magnetic resonance angiography (CE-MRA) and digital subtraction angiography (DSA)

	Vessel Conspicuity	Contrast	Vessel Continuity	Vessel Sharpness	Background Homogeneity
Relative score	−0.7 ± 1.3	0.3 ± 1.4	−1.5 ± 0.6	−1.6 ± 1.1	−1.5 ± 0.8
T^+/T^-	25.5/96.5	71/34	0/119	0/120	0/114
P value	>.05, NS	>.05, NS	<.001	<.001	<.001

Note:—A negative (positive) score indicates that DSA performs better (worse) than CE-MRA. Mean relative scores are ±1 SD. *T* values (+ or −) are based on a rank-sums test. NS indicates not significant.

this might be the ascending continuation of the AKA into the ASA, it is more likely to be venous enhancement of the AMV. Nevertheless, contribution of the ASA cannot be ruled out completely, because the ASA above the connection with the AKA may be supplied by an ARA derived from a higher thoracic or even cervical level. Moreover, the cephalad enhancement above the connection of the AKA might indeed in some instances be the ascending part of the AKA, because in 2 DSA examinations, cephalad enhancement was depicted.

DSA achieves a spatial resolution of approximately 0.2 mm, which is not yet feasible with clinical CE-MRA. This superior spatial resolution was apparent in 2 cases in which an additional ARA was found by DSA but not with CE-MRA. Anatomic literature has reported that the AKA is the largest radiculomedullary artery (diameter, 0.5–1.0 mm). In a previ-

ous study, it was shown that vessels with diameters less than or equal to 0.3 mm cannot be visualized.[8] The additional ARAs that were found by DSA (at T4 and T3 in cases 1 and 5, respectively) are therefore probably 0.3 mm or less in diameter. Moreover, the middle and upper thoracic part of the ASA has been described as difficult to image[8] because this part may suffer quite substantially from artifacts related to cardiac motion. The high spatial resolution for DSA is also demonstrated by the fact that vessel continuity and sharpnesss were significantly better when using this technique. Background inhomogeneity (eg, vertebral lipid) was stronger for CE-MRA according to the observers. DSA suffers less from this phenomenon because selective arterial injection and a subtraction technique was used to reduce background signal intensity (eg, bone). Vessel conspicuity and contrast for the AKA were found to be

equal (or even better) for CE-MRA, but the differences were not statistically significant. The 2 most important aspects that determine whether one can depict an anterior superficial spinal cord artery by CE-MRA are continuity and contrast. As explained above, the high spatial resolution obtained by DSA allows better visualization of vessel continuity. However, contrast was found to be slightly better on CE-MRA images, which is probably due to the partial volume effect, which made the anterior superficial spinal cord arteries appear wider. So, although most included patients had a spinal vascular abnormality, hampering AKA depiction, especially in case of an SDAVF with an aberrant spinal cord circulation, CE-MRA was able to correctly localize the AKA in 100% of the cases.

Visualization of the AKA by MR imaging can be of use in several clinical situations, such as preoperative work-up for thoracoabdominal aortic aneurysm surgery,[19,20] thoracoscopic spinal hernia surgery,[8] and transarterial embolization of vertebral metastases,[29] and may reduce risk for neurologic complications related to the lower spinal cord. In addition, when diagnosing SVMs, such as in SDAVF or SAVM, AKA localization by CE-MRA may have an additional precautionary contribution in that the AKA may derive from the same segmental artery as the SVM. Moreover, a number of reports[10,17,25] have demonstrated that the feeding segmental artery of an SDAVF can be localized with the use of CE-MRA.

To incorporate the described CE-MRA protocol in routine clinical practice, dedicated image postprocessing is required, and in-depth knowledge of vascular spinal cord anatomy is essential. This especially applies to cases with vascular abnormalities of the spinal cord vasculature in which the vessels may obscure the depiction of the anterior superficial spinal vasculature.

Conclusion

A noninvasive diagnostic imaging technique for visualization of the anterior superficial spinal cord arteries is of interest in several clinical situations. By validating CE-MRA against DSA, 2-phase CE-MRA was demonstrated to reliably detect and localize the AKA of the thoracolumbar spinal cord in patients with and without pathologic conditions of the spinal cord vasculature.

References

1. Kudo K, Terae S, Asano T, et al. **Anterior spinal artery and artery of Adamkiewicz detected by using multi-detector row CT.** *AJNR Am J Neuroradiol* 2003; 24:13–17
2. Takase K, Sawamura Y, Igarashi K, et al. **Demonstration of the artery of Adamkiewicz at multi-detector row helical CT.** *Radiology* 2002;223:39–45
3. Yoshioka K, Niinuma H, Ohira A, et al. **MR angiography and CT angiography of the artery of Adamkiewicz: noninvasive preoperative assessment of thoracoabdominal aortic aneurysm.** *Radiographics* 2003;23:1215–25
4. Kawaharada N, Morishita K, Fukada J, et al. **Thoracoabdominal or descending aortic aneurysm repair after preoperative demonstration of the Adamkiewicz artery by magnetic resonance angiography.** *Eur J Cardiothorac Surg* 2002;21: 970–74
5. Kawaharada N, Morishita K, Hyodoh H, et al. **Magnetic resonance angiographic localization of the artery of Adamkiewicz for spinal cord blood supply.** *Ann Thorac Surg* 2004;78:846–51; discussion 851–52
6. Yamada N, Okita Y, Minatoya K, et al. **Preoperative demonstration of the Adamkiewicz artery by magnetic resonance angiography in patients with descending or thoracoabdominal aortic aneurysms.** *Eur J Cardiothorac Surg* 2000;18:104–11
7. Yamada N, Takamiya M, Kuribayashi S, et al. **MRA of the Adamkiewicz artery: a preoperative study for thoracic aortic aneurysm.** *J Comput Assist Tomogr* 2000;24:362–68
8. Nijenhuis RJ, Leiner T, Cornips EM, et al. **Spinal cord feeding arteries at MR angiography for thoracoscopic spinal surgery: feasibility study and implications for surgical approach.** *Radiology* 2004;233:541–47
9. Bowen BC, DePrima S, Pattany PM, et al. **MR angiography of normal intradural vessels of the thoracolumbar spine.** *AJNR Am J Neuroradiol* 1996;17: 483–94
10. Farb RI, Kim JK, Willinsky RA, et al. **Spinal dural arteriovenous fistula localization with a technique of first-pass gadolinium-enhanced MR angiography: initial experience.** *Radiology* 2002;222:843–50
11. Mascalchi M, Bianchi MC, Quilici N, et al. **MR angiography of spinal vascular malformations.** *AJNR Am J Neuroradiol* 1995;16:289–97
12. Mascalchi M, Quilici N, Ferrito G, et al. **Identification of the feeding arteries of spinal vascular lesions via phase-contrast MR angiography with three-dimensional acquisition and phase display.** *AJNR Am J Neuroradiol* 1997;18:351–58
13. Mascalchi M, Cosottini M, Ferrito G, et al. **Contrast-enhanced time-resolved MR angiography of spinal vascular malformations.** *J Comput Assist Tomogr* 1999;23:341–45
14. Mascalchi M, Ferrito G, Quilici N, et al. **Spinal vascular malformations: MR angiography after treatment.** *Radiology* 2001;219:346–53
15. Pattany PM, Saraf-Lavi E, Bowen BC. **MR angiography of the spine and spinal cord.** *Top Magn Reson Imaging* 2003;14:444–60
16. Saraf-Lavi E, Bowen BC, Quencer RM, et al. **Detection of spinal dural arteriovenous fistulae with MR imaging and contrast-enhanced MR angiography: sensitivity, specificity, and prediction of vertebral level.** *AJNR Am J Neuroradiol* 2002;23:858–67
17. Shigematsu Y, Korogi Y, Yoshizumi K, et al. **Three cases of spinal dural AVF: evaluation with first-pass, gadolinium-enhanced, three-dimensional MR angiography.** *J Magn Reson Imaging* 2000;12:949–52
18. Hyodoh H, Kawaharada N, Akiba H, et al. **Usefulness of preoperative detection of artery of Adamkiewicz with dynamic contrast-enhanced MR angiography.** *Radiology* 2005;236:1004-09
19. Svensson LG. **Intraoperative identification of spinal cord blood supply during repairs of descending aorta and thoracoabdominal aorta.** *J Thorac Cardiovasc Surg* 1996;112:1455–60; discussion 1460–61
20. Williams GM, Perler BA, Burdick JF, et al. **Angiographic localization of spinal cord blood supply and its relationship to postoperative paraplegia.** *J Vasc Surg* 1991;13:23–33; discussion 33–35
21. Thron AK. **Vascular anatomy of the spinal cord.** New York: Springer-Verlag; 1988:3–5
22. Thron A. **Vascular anatomy of the spine.** In: Byrne JV, ed. *Interventional Neuroradiology*. 1st ed. Oxford: Oxford University Press; 2002:19–23
23. Zarr JH. **Biostatistical analysis.** London: Prentice Hall International Editions; 1996:163–78
24. Bowen BC, Fraser K, Kochan JP, et al. **Spinal dural arteriovenous fistulas: evaluation with MR angiography.** *AJNR Am J Neuroradiol* 1995;16:2029–43
25. Binkert CA, Kollias SS, Valavanis A. **Spinal cord vascular disease: characterization with fast three-dimensional contrast-enhanced MR angiography.** *AJNR Am J Neuroradiol* 1999;20:1785–93
26. Willinek WA, Gieseke J, Conrad R, et al. **Randomly segmented central k-space ordering in high-spatial-resolution contrast-enhanced MR angiography of the supraaortic arteries: initial experience.** *Radiology* 2002;225:583–88
27. Willinsky R, Lasjaunias P, Terbrugge K, et al. **Angiography in the investigation of spinal dural arteriovenous fistula. A protocol with application of the venous phase.** *Neuroradiology* 1990;32:114–16
28. Luetmer PH, Lane JI, Gilbertson JR, et al. **Preangiographic evaluation of spinal dural arteriovenous fistulas with elliptic centric contrast-enhanced MR angiography and effect on radiation dose and volume of iodinated contrast material.** *AJNR Am J Neuroradiol* 2005;26:711–18
29. Guzman R, Dubach-Schwizer S, Heini P, et al. **Preoperative transarterial embolization of vertebral metastases.** *Eur Spine J* 2004
30. Berenstein A, Lasjaunias P. **Spine and spinal cord vascular lesions.** In: *Surgical Neuroangiography*, Vol 5, 1st ed. Berlin: Springer-Verlag; 1992:1–85